



Residual stress of $\text{Pb}(\text{Zr}_x\text{Ti}_{1-x})\text{O}_3$ films with mixed textures

J.N. Wang^a, W.L. Li^a, B. Feng^a, C.Q. Liu^a, X.L. Li^a, Q. Sun^b, W.D. Fei^{a,*}

^a State Key Laboratory of Advance Welding Production Technology, Department of Materials Physics and Chemistry, Harbin Institute of Technology, Harbin 150001, PR China

^b School of Chemical Engineering and Technology, Harbin Institute of Technology, Harbin 150001, PR China

ARTICLE INFO

Article history:

Received 2 March 2010

Received in revised form 25 June 2010

Accepted 30 June 2010

Available online 7 July 2010

Keywords:

Sol-gel

Texture

Residual stress

Phase composition

ABSTRACT

$\text{Pb}(\text{Zr}_x\text{Ti}_{1-x})\text{O}_3$ films with different Zr/Ti ratios were prepared on Pt/Ti/SiO₂/Si substrate by sol-gel technique. By X-ray diffraction method, the residual stress of PZT films with texture was studied. The results show that there exist mixed textures with (1 1 1) and (1 0 0) textures in all the $\text{Pb}(\text{Zr}_x\text{Ti}_{1-x})\text{O}_3$ films. For the PZT films with mixed textures, residual compressive stress and tensile stress coexist in the films. The residual stress for (1 1 1)-oriented grains is compressive and that for (1 0 0)-oriented grains is tensile. The residual stress depends on both the lattice mismatch between the film and substrate and the spontaneous polarization direction of PZT films.

© 2010 Elsevier B.V. All rights reserved.

1. Introduction

$\text{Pb}(\text{Zr}_x\text{Ti}_{1-x})\text{O}_3$ (PZT) system ferroelectrics have been extensively studied because of their high piezoelectric and ferroelectric properties [1,2]. It has been shown that the properties of PZT films are influenced greatly by the Zr/Ti ratio (x value), texture and residual stress. In general, crystalline orientation and residual stress always exist in thin films [3]. For the characterization of film texture, both the relative intensity measurement [4] and rocking curve of X-ray diffraction (XRD) have been employed in previous literatures [5]. Owing to film texture is influenced by many factors, mixed textures may coexist in one film, i.e., different textures coexist in one film. In the case of mixed textures, quantitative analysis of the texture component is significant due to the strong anisotropy of PZT materials for the analysis of the film properties.

Residual stress can be induced by lattice mismatch, different coefficients of thermal expansion between film and substrate, growth stress, and so on [6–8], and affects properties [9,10] and phase transition behaviors of ferroelectric films [11–13]. In the various methods for the characterization of residual stress of the films, the XRD method is the most convenient and accurate. Some theories [14–16] of residual stress measurement using XRD have been put forward on the basis of Reuss [17] and Voigt [18] conditions. The characterization of residual stress using XRD is complex because of the existence of texture and grain interaction in polycrystalline

films. On the basis of various grain interaction models, the residual stress in films with single texture has been characterized [15,16]. However, few studies have been reported on the residual stress in films with mixed textures.

In the present study, we report that mixed textures can be formed in PZT films with different Zr/Ti ratios on the highly (1 1 1)-oriented Pt substrate. The residual stress and mixed textures are investigated by XRD method, and the relationship between the residual stress and mixed textures is also discussed.

2. Experimental

Films used in this study were prepared on the highly (111)-oriented Pt/Ti/SiO₂/Si substrate using sol-gel method. Lead acetate trihydrate, zirconium *n* propoxide and titanium isopropoxide were used as raw materials and 2-methoxyethanol [2-CH₃OCH₂CH₂OH] as the solvent. The 10 mol% excess Pb solution was used to overcompensate for any Pb loss during high temperature annealing, and the Zr/Ti ratios were controlled as 51/49, 52/48, 54/46, 55/45, and 58/42, respectively. The concentration of final solution of PZT can be diluted to 0.4 M. The PZT precursor solution was firstly spin-coated on the substrate with the spin rate of 4000 rpm for 9 s, and then the wet films were pyrolyzed at 500 °C on a plate-hot for 2 min. The above two processes were repeated for seven times to attain the desired film thickness. Finally, the films were crystallized at 650 °C for 3 min through rapid thermal annealing technique in O₂ ambient. The thickness of PZT films is about 350 nm, and the size of samples is 10 mm × 10 mm. Pt dots as top electrodes with the diameter of 0.2 mm were deposited on the surface of films using magnetron sputtering system in Ar ambient.

To characterize the phase composition, texture and residual stress of PZT films, the θ - 2θ scan, ω scan and ψ scan XRD were carried out on Philips X'pert diffractometer with Cu K α radiation. During the measurement of X-ray Diffraction, X-ray beam size is 2 mm in width and 8 mm in length. The scheme of optics is shown in Fig. 1, and there is no changing of X-ray optics in the measurement process of all samples. In addition, the (1 1 0) peaks at different ψ were correct by the powder diffraction.

* Corresponding author. Tel.: +86 451 86418647; fax: +86 451 86418647.
E-mail address: wdfei@hit.edu.cn (W.D. Fei).

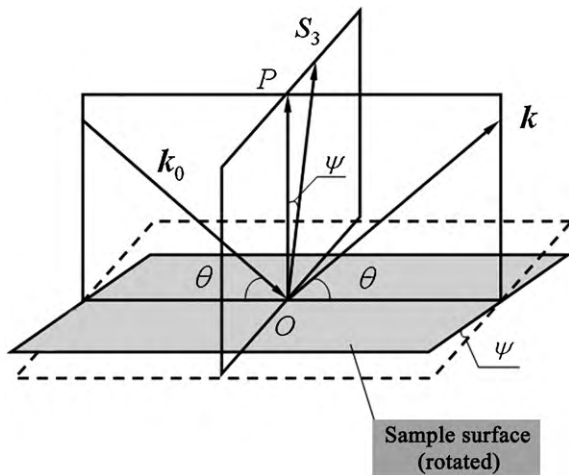


Fig. 1. Schematic diagram of ψ -scan XRD. In a given tilt angle (ψ), the (1 1 0) diffraction peak was measured using θ - 2θ scan XRD.

3. Results and discussion

3.1. Phase composition and texture

The phase compositions of PZT films with different Zr/Ti ratios are investigated using θ - 2θ scan XRD, and the results are presented in Fig. 2. It can be seen that all films are composed of pure perovskite phase, and no other phase can be found in the XRD curves. For convenient discussion, the perovskite phase in all films is indexed with respect to pseudocubic coordinate system. From Fig. 2, only (1 0 0) and (1 1 1) diffractions of the PZT films can be seen and the intensities of the two diffractions are very high, which implies that the preferred orientations along (1 0 0) and (1 1 1) directions coexist in PZT films, i.e., there exist mixed textures in PZT films.

The angle (α) between lattice planes ($h_1 k_1 l_1$) and ($h_2 k_2 l_2$) in cubic coordinate system can be calculated by the following equation:

$$\cos \alpha = \frac{h_1 h_2 + k_1 k_2 + l_1 l_2}{\sqrt{h_1^2 + k_1^2 + l_1^2} \sqrt{h_2^2 + k_2^2 + l_2^2}} \quad (1)$$

According to the equation, the angle between (1 1 0) and (1 1 1) planes is about 35° , and it is about 45° between (1 1 0) and (1 0 0) planes. In order to quantitatively analyze the mixed textures in PZT films, (1 1 0) diffractions of PZT films at different tilt angles (ψ) were measured (denoted as ψ -scan XRD, ψ is the angle between the normal of diffraction plane and normal of the films). For the case of the

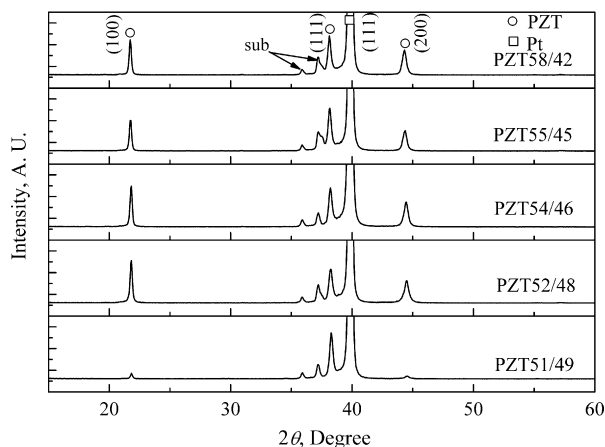


Fig. 2. θ - 2θ scan XRD curves of PZT films with different Zr/Ti ratios.

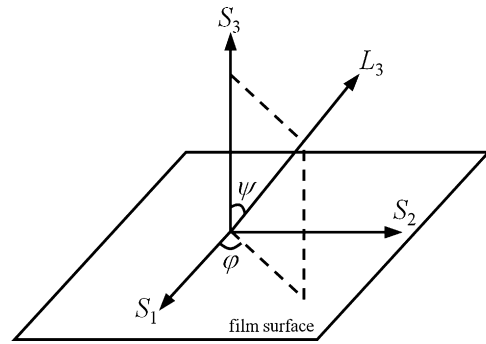


Fig. 3. Relationship between the film coordinates ($O-S_1S_2S_3$) and experimental coordinates ($O-L_1L_2L_3$).

(1 1 1) texture, (1 1 0) plane normal direction is distributed on the generatrices of the cone with the ψ angle of about 35° to the S_3 axis (S_3 shown in Fig. 3 represents the normal of the film surface), and about 45° for the case of the (1 0 0) texture [19]. When ψ is about 35° , the XRD peak intensity of (1 1 0) plane is proportion to the orientation probability of (1 1 1) plane, and that is corresponding to the orientation probability of (1 0 0) plane for ψ angle of 45° [19]. According to the above analysis, the integral intensity (I_ψ)- $\sin^2 \psi$ curve must exhibit two peaks at about $\psi = 35^\circ$ and $\psi = 45^\circ$, if (1 1 1) and (1 0 0) textures coexist in the film. As shown in Fig. 4, two peaks can be clearly found in I_ψ - $\sin^2 \psi$ curves at about $\psi = 35^\circ$ and $\psi = 45^\circ$ for all films, which confirms that both (1 1 1) and (1 0 0) textures coexist in PZT films. In Fig. 4, it can be found that the (1 1 1) texture is dominant in PZT films (owing to the higher intensity at about ψ angle of 35°). In addition, the content of (1 0 0)-oriented grains in PZT films are shown in Fig. 5, which is calculated from Gauss fitting of I_ψ - ψ curves (not shown in the present study). In Fig. 5, $I_{\psi-35}$ and $I_{\psi-45}$ are defined as integral intensity of Gauss fitting peaks at about ψ angles of 35° and 45° in I_ψ - ψ curves, respectively. From Fig. 5, it can be seen that the content of (1 0 0)-oriented grains increases roughly with the Zr/Ti ratio increasing. Because the lattice mismatch of the atom arrangements between (1 1 1) plane of PZT and (1 1 1) plane of Pt is only 2.8% [20], (1 1 1) texture in PZT film can be induced by (1 1 1) oriented Pt substrate. In addition, (1 0 0) texture has also been found on (1 1 1)-oriented Pt substrate by some authors [21–23], which suggests that the (1 0 0)_{PZT}/(1 1 1)_{Pt} is possible in point of interface energy.

3.2. Residual stress

To characterize the residual stress in PZT films, interplaner spacing of PZT (1 1 0) planes at different tilt angle ψ were measured, which is defined as d_ψ . Because both (1 1 1) and (1 0 0) textures coexist in PZT films, the (1 1 0) diffraction with higher intensity and well shape can be obtained at the ψ angle of 25 – 50° . The d_ψ - $\sin^2 \psi$ curves for PZT films with different Zr/Ti ratios are shown in Fig. 4, and the non-monotonic relationship between d_ψ and $\sin^2 \psi$ can be clearly seen. In general, d_ψ - $\sin^2 \psi$ curve is used to the analysis of residual stress on the base of various grain interaction models, and monotonous increasing/decreasing of the d_ψ - $\sin^2 \psi$ curve is corresponding to tensile/compressive stress in the films. In Fig. 4, it can be found that the linear decreasing fraction of the d_ψ - $\sin^2 \psi$ relations are mainly corresponding to the (1 1 1)-oriented grains and the linear increasing fraction are mainly corresponding to the (1 0 0)-oriented grains. The non-monotonic relationships in d_ψ - $\sin^2 \psi$ curves may be caused by following reasons. The lattice mismatch between (1 1 1)_{PZT} and (1 1 1)_{Pt} can induce compressive stress in (1 1 1)-oriented PZT grains in the sample frame. For (1 0 0)-oriented grains, lattice mismatch between (1 0 0)_{PZT} and (1 1 1)_{Pt} is complex, the residual stress tend to be balance with that in (1 1 1)-

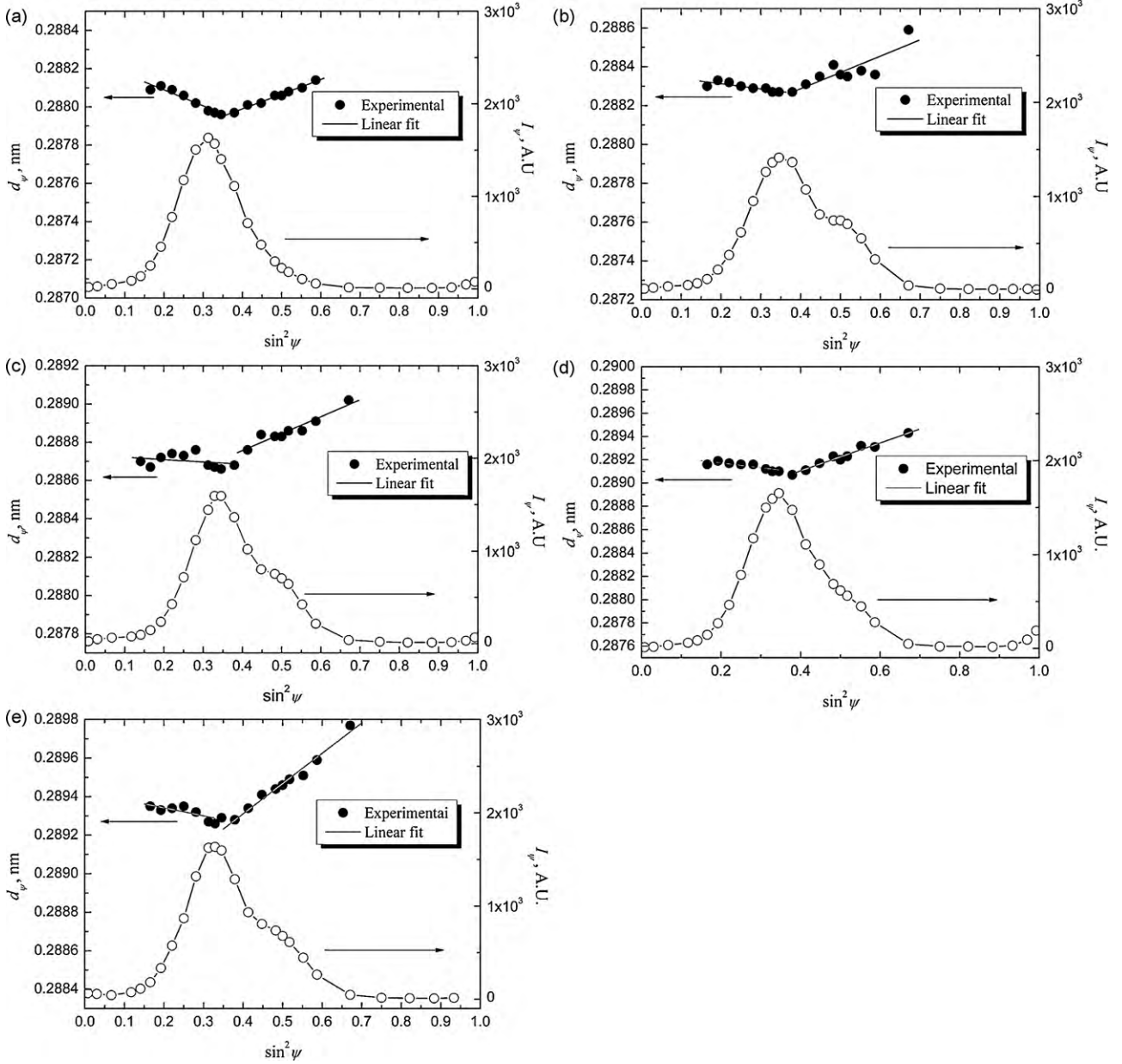


Fig. 4. Integral intensity of (110) diffraction peak characterized by $\theta-2\theta$ scan and interplaner spacing (d_ψ) at different tilt angle ψ as functions of $\sin^2\psi$, (a) $x=0.51$, (b) $x=0.52$, (c) $x=0.54$, (d) $x=0.55$, and (e) $x=0.58$.

oriented grains in point of elastic energy, so the residual stress of (100)-oriented grains in the sample frame may be tensile. Because the residual stress in PZT films is closely related to the lattice mismatch, Voigt [18] model can be employed to analyze the residual stress for both (111)- and (100)-oriented grains.

For the simplification, the textures in PZT films are assumed as ideal ones, i.e., the misorientation of the textures is ignored. We assume that all grains with the same orientation have the same strain tensor in $O-S_1S_2S_3$ system [19]. According to Voigt model, when the crystal structure is simplified as cubic and (110) plane is given as measurement plane, the relationship between strain ε and stress σ can be calculated from the following equation [16]:

$$\varepsilon_{\varphi\psi} = \sum_{i,j} F_{ij}(\varphi, \psi) \langle \sigma_{ij}^S \rangle_{\varphi\psi}, \quad i, j = 1, 2, 3 \quad (2)$$

where φ and ψ are the azimuth angles of the L_3 axis of the $O-L_1L_2L_3$ coordinates (experimental coordinates) in $O-S_1S_2S_3$ coordinates, L_3 axis is parallel to the normal direction of the measured (110) plane, as shown in Fig. 3. $\langle \rangle$ represents the average for all grains with the same orientation, and σ_{ij}^S is the stress tensor. The meaning of $F_{ij}(\varphi, \psi)$ is an orientation distribution function (ODF), and it is the same with that in Ref. [16]. In the case of ideal texture, the ODF can be assumed as Dirac's delta function, and Eq. (2) can be simplified greatly. Because the average stress in the film is axis symmetry to S_3 axis, Eq. (2) can be simplified as

$$\varepsilon_\psi = \varepsilon_0 + M\sigma_{\parallel}^S \sin^2 \psi \quad (3)$$

where ε_ψ is the strain measured at the tilt angle ψ , constant M is related to the elastic coefficient of PZT ceramics, and σ_{\parallel}^S is the average stress parallel to the film surface for (111)-oriented and (100)-oriented grains in the sample frame. Because M is related to the orientation, M values are different for different oriented grains.

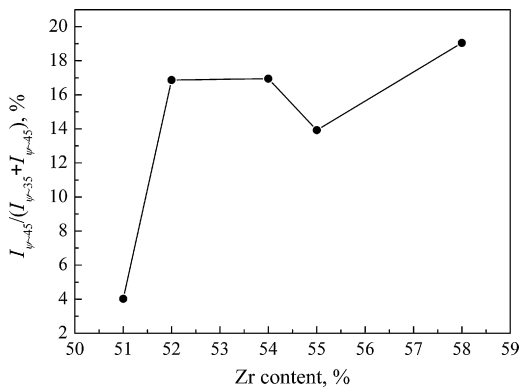


Fig. 5. Relationship between the content of (100)-oriented grains and Zr/Ti ratios.

Based on the elastic coefficients given in Ref. [24], the M values can be calculated for PZT with $x = 0.52$, and M is 0.324×10^{-10} /Pa for (111)-oriented grains, and 0.260×10^{-10} /Pa for (100)-oriented grains. Eq. (3) can be written as follows:

$$d_{\psi} = d_0 \varepsilon_0 + d_0 M \sigma_{\parallel}^S \sin^2 \psi = d_0 \varepsilon_0 + M' \sigma_{\parallel}^S \sin^2 \psi \quad (4)$$

where d_0 is the lattice constant of stress free sample, and $M' = Md_0$. It is clear that the slope of $d_{\psi} - \sin^2 \psi$ curve is constant for both (111)- and (100)-oriented grains. Therefore,

$$\sigma_{\parallel}^S = \frac{K}{M'} \quad (5)$$

where $K = \partial d_{\psi} / \partial \sin^2 \psi$ is the slope of $d_{\psi} - \sin^2 \psi$ curve. The M' values of PZT is only related to its elastic constants for ideal texture, and the changes of elastic constants in the range of $x = 0.51$ – 0.58 are not big according to the reference [25]. As a qualitative comparison, the difference of M' values for PZT films with different x values can be negligible in the present study. Therefore, the K value represents the magnitude of the residual stress in every PZT film, and the K as the function of x value is shown in Fig. 6. It can be clearly found that the residual stress is compressive in (111)-oriented grains and tensile in (100)-oriented grains. As shown in Fig. 6, with x increasing, the compressive residual stress in (111)-oriented grains decreases when $x \leq 0.54$, increases at the range of $0.54 \leq x \leq 0.55$, and tends to be almost changeless when $x \geq 0.55$. The tensile stress in (100)-oriented grains increases with x increasing.

To understand the changing tendency of residual stress in (111)-oriented grains, the spontaneous polarization directions of different phases and the lattice mismatch between PZT and Pt must be taken into account. For the first one, according to PbTiO_3 – PbZrO_3 phase diagram [26,27], R phase with rhombohedra structure in the Zr-rich region (spontaneous polarization along [111] direction) and T phase with tetragonal structure in

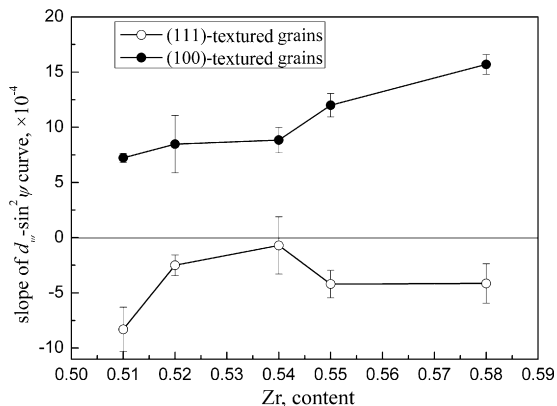


Fig. 6. Slope of $d_{\psi} - \sin^2 \psi$ curve as functions of x value.

the Ti-rich region (spontaneous polarization along [001] direction) are separated by a morphotropic phase boundary (MPB). In the vicinity of MPB ($x \approx 0.52$ – 0.54 at 300K), M phase with monoclinic structure has been confirmed by many studies [28–30]. Because the spontaneous polarization of M phase can rotate from [001] to [111] directions in $(\bar{1}10)$ plane, the spontaneous polarization of PZT rotates from [001] direction to [111] direction when x increases from 0.51 to 0.58. When PZT films are cooled from high temperature, the phase transition from paraelectric state to ferroelectric state must take place. The spontaneous polarization along [111] direction means that the elongation of lattice structure is along [111], so this type spontaneous polarization can reduce the compressive stress of (111)-oriented grains. Therefore, we can deduce that the compressive stress in PZT films with (111) texture can be relaxed by the spontaneous polarization along [111]. For the second one, because the atomic radius of Zr is larger than that of Ti, the compressive stress in (111)-oriented grains can increase with Zr content increasing. For PZT films with $x \leq 0.54$, the decreasing compressive stress may be dominated by the change of the spontaneous polarization direction rather than the increasing lattice mismatch between PZT and Pt with Zr content increasing. For PZT films with $x \geq 0.54$, the main reason why the compressive stress increases at high x value is converse.

Because the content of (100)-oriented grains is less compared with that of (111)-oriented grains in PZT films, the tensile stress in (100)-oriented grains may be mainly determined by stress balance tendency between the two oriented grains. In this case, the tensile stress in (100)-oriented grains exhibits generally the similar behavior compared with compressive stress in (111)-oriented grains with x value increasing.

But in PZT films with the range of $x = 0.51$ – 0.54 , the tensile stress of (100)-oriented grains increases monotonously, which is not in accordance with compressive stress of (111)-oriented grains. Although the stress balance between the two oriented grains can affect the residual stress, it is not the unique factor to affect the residual stress, because the residual stress is also affected greatly by the substrate. In addition, the spontaneous polarization in ferroelectric film can also affect the residual stress. According to the discussion mentioned above, the PZT51/49 locates at the tetragonal phase region with the spontaneous polarization direction along [001], so the polarization in (100)-oriented grains can relax greatly the tensile residual stress of the grains, correspondingly, the tensile stress in the (100)-oriented grains is relative low.

PZT52/48 and PZT54/46 are located in the vicinity of MPB, and M phase can exist in the films. The spontaneous polarization direction of M phase lies in $(\bar{1}10)$ plane between [001] and [111]. That is to say, the spontaneous polarization of M phase in (100)-oriented grains is not in-plane, so the relaxation effect of polarization on the tensile stress in (100)-oriented grains is smaller than that in the PZT51/49 film.

4. Conclusions

By sol-gel technique, the highly oriented PZT films with different Zr/Ti ratios can be obtained on highly (111)-oriented Pt substrate. The films are found to be mixed textures combined with (111) and (100) orientations, and the main texture is (111). With the x value increasing, the content of (100)-oriented grains increases roughly. It is found that the residual stress in (111)-oriented PZT grains is compressive, and that in (100)-oriented grains is tensile. The changing tendency of residual compressive stress in (111)-oriented grains and residual tensile stress in (100)-oriented grains exhibits the similar behavior with x value increasing.

References

- [1] K. Uchino, *Piezoelectric Actuators and Ultrasonic Motors*, Kluwer Academic, Boston, 1996.
- [2] I.A. Kornev, L. Bellaiche, P.-E. Janolin, B. Dkhil, E. Suard, *Phys. Rev. Lett.* 97 (2006) 157601.
- [3] L.B. Freund, S. Suresh, *Thin Film Materials: Stress, Defect Formation and Surface Evolution*, Cambridge University Press, 2003.
- [4] D.A. Hall, A. Steuwer, B. Cherdhirunkorn, T. Mori, P.J. Withers, *Acta Mater.* 54 (2006) 3075–3083.
- [5] F. Yang, W.D. Fei, *Key Eng. Mater.* 280–283 (2005) 857–860.
- [6] D.E. Jesson, S.J. Pennycook, J.M. Baribeau, *Phys. Rev. Lett.* 66 (1991) 750–753.
- [7] J.A. Floro, S.J. Hearne, J.A. Hunter, P. Kotula, E. Chason, S.C. Seel, C.V. Thompson, *J. Appl. Lett.* 89 (2001) 4886–4897.
- [8] M.F. Doerner, W.D. Nix, *CRC Crit. Rev. Solid State Mater. Sci.* 14 (1988) 225–268.
- [9] C.Q. Liu, W.D. Fei, W.L. Li, *J. Phys. D: Appl. Phys.* 41 (2008) 125404.
- [10] J.W. Lee, G.T. Park, C.S. Park, H.E. Kim, *Appl. Phys. Lett.* 88 (2006) 072908.
- [11] N.A. Pertsev, V.G. Kukhar, H. Kohlstedt, R. Waser, *Phys. Rev. B* 67 (2003) 054107.
- [12] C.Q. Liu, W.D. Fei, W.L. Li, *Thin Solid Film* 516 (2008) 1265–1270.
- [13] S.H. Oh, H.M. Jang, *J. Appl. Phys.* 85 (1999) 2815–2820.
- [14] L. Meda, K.H. Dahmen, S. Hayek, H. Garmestani, *J. Cryst. Growth* 263 (2004) 185–191.
- [15] G. Abadias, Y.Y. Tse, *J. Appl. Phys.* 95 (2005) 2414–2428.
- [16] M.V. Leeuwen, J.D. Kamminga, E.J. Mittemeijer, *J. Appl. Phys.* 86 (1999) 1904–1914.
- [17] A. Reuss, *Z. Angew. Math Mech.* 9 (1929) 49–58.
- [18] W. Voigt, *Lehrbuch der Kristallphysik*, Leipzig, Teubner, 1910, p. 369.
- [19] W.D. Fei, C.Q. Liu, M.H. Ding, W.L. Li, L.D. Wang, *Rev. Sci. Instrum.* 80 (2009) 093903.
- [20] Z. Huang, Q. Zhang, R.W. Whatmore, *J. Appl. Phys.* 85 (1999) 7355–7361.
- [21] L. Lian, N.R. Sottos, *J. Appl. Phys.* 87 (2000) 3941–3949.
- [22] S.Y. Chen, C.L. Sun, *J. Appl. Phys.* 90 (2001) 2970–2974.
- [23] B.G. Chae, Y.S. Yang, S.H. Lee, M.S. Jang, S.J. Lee, S.H. Kim, W.S. Baek, S.C. Kwon, *Thin Solid Film* 410 (2002) 107–113.
- [24] X.J. Zheng, Y.C. Zhou, J.Y. Li, *Acta Mater.* 51 (2003) 3985–3997.
- [25] D.A. Berlincourt, C. Cmluk, H. Jaffe, *Proc. IRE* 48 (1960) 220–229.
- [26] B. Noheda, D.E. Cox, G. Shirane, R. Guo, B. Jones, L.E. Cross, *Phys. Rev. B* 63 (2000) 014103.
- [27] I.A. Kornev, L. Bellaiche, P.E. Janolin, B. Dkhil, E. Suard, *Phys. Rev. Lett.* 97 (2006) 157601.
- [28] E.B. Araújo, E.C. Lima, J.D.S.A. Guerra, O. dos Santos, L.P. Cardoso, M.U. Kleinke, *J. Phys.: Condens. Matter* 20 (2008) 415203.
- [29] A.K. Singh, D. Pandey, S. Yoon, S. Baik, N. Shin, *Appl. Phys. Lett.* 91 (2007) 192904.
- [30] J. Rouquette, J. Haines, V. Bornand, M. Pintard, Ph. Papet, W.G. Marshall, S. Hull, *Phys. Rev. B* 71 (2005) 024112.